Journal of Current Research in Oral Surgery
2025, Volume 5, Issue 2, Page No: 39-50

Available online at: www.tsdp.net

ISSN: 3062-3480

Original Article

Accuracy and Agreement of Vertical Bone Height Measurements: A Comparative Study of Panoramic Radiography and CBCT

Claire Martin[1], Julien Robert[2]*, Sophie Bernard[1], Antoine Girard[2]

[1]Department of Oral and Dental Surgery, Faculty of Dentistry, University of Lyon, Lyon, France.
[2]Department of Clinical Oral Sciences, Faculty of Medicine, University of Strasbourg, Strasbourg, France.

***E-mail** ✉ julien.robert@gmail.com

Received: 03 April 2025; **Revised:** 16 July 2025; **Accepted:** 16 July 2025

ABSTRACT

The present study aimed to determine which imaging modality—panoramic radiography (PAN) or cone-beam computed tomography (CBCT)—yields superior accuracy for vertical measurements in the maxillary posterior region. Anatomically matched locations across the maxillary posterior area were identified on both PAN and CBCT records and subjected to vertical assessment. The quantity measured was the linear distance extending from the osseous crest to the inferior boundary of the maxillary sinus cavity. Toothless segments underwent measurement following an identical protocol. Where a defect could be discerned, its vertical magnitude was separately quantified. The resulting dataset underwent statistical analysis. Pairwise comparison of matched sites on CBCT and PAN images yielded a cohort of 204 individuals, of whom 341 discrete measurements (n = 341) satisfied the enrolment criteria. Pooled mean values registered at 7.21 ± 3.74 mm using PAN and 7.62 ± 4.06 mm using CBCT. The average departure between paired readings was −0.41 ± 1.03 mm. The observed discrepancy between PAN- and CBCT-derived values was statistically significant ($P < 0.001$). Detectable defects were present at 58 of the 341 measurement sites (17%). Mean vertical extent of these defects measured 1.85 ± 1.05 mm on PAN versus 1.99 ± 1.00 mm on CBCT. Defect height comparisons did not attain statistical significance ($P = 0.052$). Despite a statistically demonstrable offset of −0.41 ± 1.03 mm emerging across all paired observations when juxtaposing PAN against CBCT vertical height readings, the magnitude of this offset proves clinically trivial upon consideration. Either PAN or CBCT constitutes a valid approach for ascertaining vertical bone dimensions in the posterior maxilla.

Keywords: Bone height measurements maxilla, Cone beam computerized tomography, Vertical distances CBCT/panoramic radiography, Alveolar height depiction CBCT, Vertical measurements posterior maxilla, Comparison panoramic radiograph and CBCT

How to Cite This Article: Martin C, Robert J, Bernard S, Girard A. Accuracy and Agreement of Vertical Bone Height Measurements: A Comparative Study of Panoramic Radiography and CBCT. J Curr Res Oral Surg. 2025;5(2):39-50. https://doi.org/10.51847/eKZrAIuYXz

Introduction

Tooth loss and subsequent extraction set in motion a cascade of horizontal and vertical hard-tissue diminutions that distort the native topography of the alveolar process. Degradation of the underlying bony scaffold triggers concomitant soft-tissue collapse, thereby undermining both the cosmetic appearance and the potential for biological integration [1]. **Figure 1** captures the clinical presentation of vertical osseous deformities both prior to and following implant-supported prosthodontic rehabilitation **(Figure 1).** An additional predicament stems from the stepped contour of vertical bone loss, which, in turn, impedes effective oral hygiene maintenance.

a)

b)

Figure 1. Clinical images showing vertical defects in edentulous jaw sections in regions 26–28 before (a) and after treatment (b).

Insufficient residual ridge stature, along with irregularities in ridge contour, stand out as the foremost obstacles constraining reconstructive efforts in the posterior maxillary quadrant [2]. Maxillary sinus floor augmentation is commonly advocated when implant-retained prostheses are planned. The technique enjoys a reputation as an efficacious and dependable method for site development in the atrophic posterior maxilla, delivering the prerequisite osseous volume for fixture placement [3-5]. All the same, the intervention introduces operative hazards, not least inadvertent tearing of the Schneiderian membrane or hemorrhagic events traceable to vascular injury [6].

Notwithstanding the procedure's predictability and favorable long-term survival figures, a range of intra- and postoperative adverse events has been reported in the literature [7]. Among these, trauma to blood vessels is capable of eliciting considerable bleeding features prominently [8]. Uncontrolled hemorrhage stemming from iatrogenic disruption of the alveolar antral artery (AAA) is, in conjunction with sinus membrane perforation, counted among the two principal adverse events of sinus lifting (SL) procedures [9].

Taking an alternative perspective, newly emerging data suggest that even short-length implants may offer a perfectly tenable solution for achieving enduring, successful oral rehabilitation once teeth have been lost [7, 8]. Turning to short implants confers multiple advantages upon both patients and treating clinicians, chief among them being reduced procedural morbidity, decreased economic outlay, and a substantially shortened overall course of therapy [8, 9].

Figure 2 reproduces radiographic documentation of short implants seated in region 26 directly after prosthetic component delivery (A) and at a three-year post-restoration recall (B). The presence of the short implant at site 26 rendered any supplementary augmentation unnecessary **(Figure 2).**

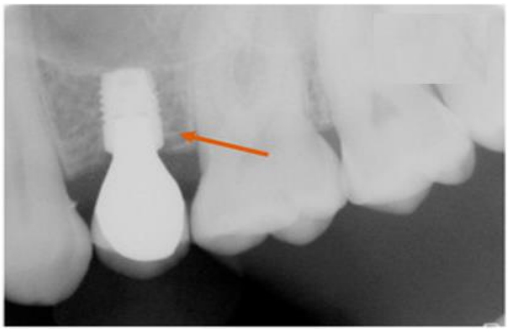

a)

b)

Figure 2. X-ray images of short implants in region 24 after prosthetic insertion (a) and 1 year after prosthetic restoration (b). Orange arrows mark the implant with adapted peri-implant bone.

At its core, the three-dimensional spatial placement of an implant is a decisive parameter that directly governs the design of the final prosthetic superstructure, shaping the contours of the emergence profile [10].

The apicocoronal coordinate of implant placement is no less consequential, as sufficient vertical clearance is an indispensable condition for sculpting an optimal transmucosal transition zone, achieving pleasing gingival contours, and fashioning a lifelike clinical crown anatomy [11].

Adequate clearance must be pre-planned to foster the maturation of sound peri-implant soft tissues, entailing a mucosal thickness of 3–4 mm and a zone of keratinized attached gingiva at least 2 mm wide [12, 13].

Standard recommendations emphasize the need to perform a meticulous radiologic survey of the maxillary anatomy before any surgical maneuvers to avoid foreseeable complications [14, 15].

For successful diagnostic workup within the disciplines of oral and maxillofacial surgery as well as for comprehensive pre-surgical strategizing, both panoramic radiography (PAN) and cone-beam computed tomography (CBCT) are employed to great advantage [16-18]. A considerable number of investigations have attested to the relative diagnostic advantage of CBCT over PAN when the task involves distinguishing key anatomic landmarks and blueprinting implant insertions targeting the maxilla [19-21].

Although acquiring reliable vertical dimensional data lies at the heart of clinical deliberations regarding implant surgery in the posterior maxilla, the extent to which measurements from PAN images are interchangeable with those from CBCT remains an under-researched question. The outcomes of the present study might therefore inform practical, everyday clinical judgment.

The central aim driving this investigation was to establish whether the vertical distance (VD) separating the osseous peak at the first molar site from the floor of the maxillary sinus reads comparably when derived from paired panoramic radiographic (PAN) versus cone-beam computed tomographic (CBCT) records.

Measurement procedures were also applied to study participants presenting with either total edentulism or tooth loss confined exclusively to the predetermined region of interest.

In those instances where vertical bone defects were discernible within the demarcated zone, their corresponding vertical magnitude (defect height, DH) was captured on both PAN and CBCT depictions in addition to the aforementioned primary measurements.

The central premise tested was that no measurable discrepancy would emerge between CBCT and their correlated PAN counterparts when evaluating both VD and DH.

Materials and Methods

The Committee of the Baden granted ethical clearance for this investigation–Württemberg Medical Association (F-2014-006-z), and the work was executed in full compliance with the ethical framework outlined in the 1964 Declaration of Helsinki [22]. An exhaustive account of the methodology governing panoramic and cone-beam computed tomographic image selection, the uniform measurement workflow, examination environment specifications, the designated software package and display monitor, and the examiner's level of training can be located within the Materials and Methods segment of the publication by Ketabi *et al*. [21].

A starting cohort of 549 individuals was identified for potential enrolment by searching the archival records of a dental practice in Stuttgart, Germany, which had been referred for both PAN and CBCT scans during the period from February 2010 to January 2017. Critically, both imaging datasets were already stored and accessible before the research formally commenced.

For analytical purposes, those PAN and CBCT acquisitions **(Figure 3)** that depicted at least one matching maxillary hemiarch were selected. The magnification coefficient inherent to the panoramic apparatus had been ascertained at the time of radiographic unit installation, by imaging a series of reference standards whose true dimensions were already documented—these included both spherical calibration markers and cylindrical titanium benchmarks. Informed by these calibration trials, a compensatory magnification multiplier of 1.25 was computed and then uniformly deployed herein to rectify the panoramic images. Consistent yearly servicing, together with periodic recalibration assessments, was carried out to maintain measurement fidelity. At the time the study was undertaken, the Stuttgart practice's imaging repository contained radiographic files for 549 patients. Among these, 64 had originated from outside imaging centers. Given that calibrated reference items of known geometry (such as titanium cylinders or calibration spheres) were present in upwards of 70% of these scans, these images were deemed admissible and retained in the study dataset.

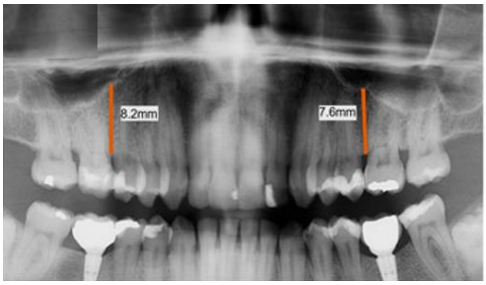

a)

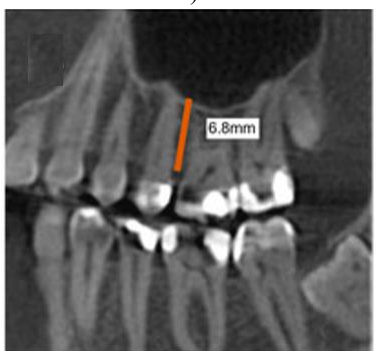

b)

Figure 3. (a) PAN image of the maxilla showing vertical height measurements in region M1, right

and left. (b) CBCT image of the maxilla with measurement on the sagittal slice. The orange bars show examples of the measuring points in PAN (left) and CBCT (right).

Adopting this inclusive strategy also enabled the incorporation of PAN radiographs that lacked a dimensional reference marker.

The primary measurement captured was the linear vertical interval originating at the mesial osseous peak overlying the first molar (M1) and terminating at the inferior border of the maxillary sinus **(Figure 3).** If the M1 region did not lend itself to measurement, an alternate posterior maxillary locale (M2) was substituted.

When dealing with patients who were either fully toothless or edentulous strictly within the region of interest and presented with no discernible vertical osseous craters, a tailored technique was applied. Specifically, a reference guideline was digitally superimposed to intersect two reliably identifiable anatomic points situated along the alveolar crest. The determination of the measurement span relied upon geometric construction: the perpendicular distance dropped from this reference guideline down to the floor of the sinus was taken as the vertical measurement **(Figure 4a)**. Employing this geometrical strategy helps bolster reproducibility while reducing the likelihood of measurement error.

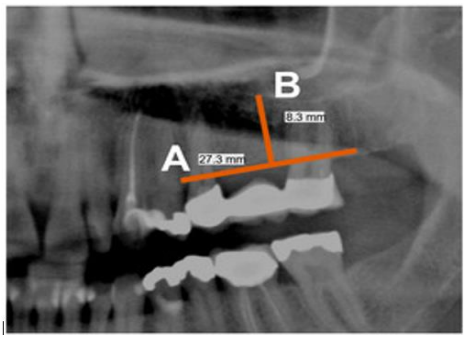

a)

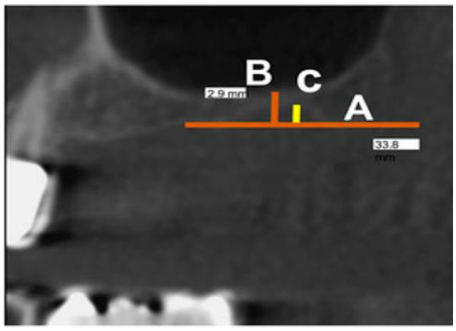

b)

Figure 4. (a) PAN image of the maxilla without vertical defects showing the measurement in the edentulous region of the auxiliary line (A) and the perpendicularly formed line (B) on this plane. (b) CBCT image of the maxilla with vertical defects showing measurement of the auxiliary line (A) and the perpendicularly formed line (B) on this plane, as well as the defect height (C).

For scenarios with vertical ridge deficiencies within the stipulated region, an analogous approach was pursued. Over and above the primary measurement segment already delineated, any vertical bone defect arising post-extraction was likewise quantified as a geometrically derived perpendicular span reaching from the superimposed reference guideline upward to the most coronal extent of the defect concavity **(Figure 4b)**.

To qualify for measurement inclusion, scans needed to satisfy the following conditions:

- Image acquisition dates falling between February 2010 and January 2017;
- Proper and consistent alignment of the patient's head during exposure;
- Easily identifiable, reliably relocalizable anatomic landmarks are visible across both imaging platforms.

Participants were withdrawn from the study provided that, within the designated measurement field on either or both radiographic modalities, any of the circumstances below were met:

- Periapical radiolucencies, recent extraction sockets, augmented sites, or existing implant fixtures were noted.
- A discrepancy in dental status between the PAN and CBCT records was evident.
- Alterations in alveolar ridge contour or irregularities of the antral floor anatomy were identified.
- Periodontal bony defects were observable.
- Image-degrading artifacts (exemplified by metallic restorations superimposing the crestal ridge) were detected.

The workflow was organized so that diagnostic interpretation was first rendered on the PAN studies, followed by the independent interpretive assessment of the matched CBCT volumes. Staging the readings in this order was deliberately intended to eliminate any risk that observations made on the PAN views could bias the evaluation of the CBCT datasets. All radiographic appraisals were performed by a single examiner who, ahead of the study launch, had undergone targeted instruction and competence

verification delivered by a specialist with recognized expertise in dental and maxillofacial radiology. To establish measurement trustworthiness, replicate readings were performed on scans of 25 randomly selected subjects (25 CBCT volumes and 25 PAN radiographs). Inter-rater agreement levels were defined by contrasting measurement output between the primary examiner and the supervising specialist. In contrast, intra-rater consistency was computed by having the same examiner reassess each study image a second time after a 14-day interval.

Data capture was undertaken using custom-built research software, with all subsequent statistical computations being carried out by MediStat GmbH (SPSS Statistics 25, IBM Corporation, Armonk, NY, USA).

Reported outcomes for exploratory and descriptive parameters are presented as raw numerical counts.

Assessment of intra-rater repeatability was conducted using a paired-samples test, juxtaposing readings from the first session against those from the second. Hypothesis testing employed a two-sided paired-samples framework to explore the bidirectional association between PAN- and CBCT-derived measurements. As a supplementary metric, the effect sizes corresponding to the paired sample comparisons were expressed in terms of Cohen's d. The tightness of the linear relationship between PAN and CBCT readings was quantified using the Bravais–Pearson correlation coefficient. In situations where the observed data demonstrated wide variability and non-normality, the Wilcoxon matched-pairs signed-rank test was used as the nonparametric analog.

A computed p-value equal to or falling below 0.05 was interpreted as denoting a statistically meaningful difference.

Results and Discussion

The final sample, meeting all eligibility requirements, consisted of 204 individuals, including 111 females and 93 males. The mean age among female participants was 55.9 years, whereas it was 52.9 years among male participants. The degree of inter-observer dependability and precision was documented at 99.4%. Regarding intra-rater consistency, vertical measurements recorded at two distinct time points were compared using a paired-samples t-test. "T-PAN" captures the variation between repeated vertical distance readings obtained from panoramic images (n = 37), whilst "T-CBCT" captures the variation between repeated readings obtained from cone-beam computed tomographic volumes (n = 37). For T-PAN and T-CBCT, the mean paired divergences were −0.140 mm and 0.023 mm, respectively. Neither comparison yielded a statistically significant difference between the two recording sessions ($P \geq 0.05$), with two-sided p-values of $P = 0.179$ for T-PAN and $P = 0.334$ for T-CBCT.

A cumulative set of 341 (n = 341) matched measurement pairs was collated from PAN and CBCT imaging, comprising 175 derived from the right maxilla (n = 175) and 166 from the left maxilla (n = 166).

The measurement outputs for vertical dimensions are presented visually in **Figure 5** as scatterplots. These graphical depictions illustrate how the vertical distances extracted from panoramic radiographs (PAN) correspond to those yielded by CBCT scans. The identity line (shown in red) depicts the hypothetical condition of perfect concordance, where coordinate pairs on both axes coincide exactly (y = x). The fitted regression trajectory (drawn in blue) sketches the empirical interrelation between the PAN- and CBCT-derived measurement collections. As shown in the graph, the regression curve computed across the entire dataset lies consistently above the identity line.

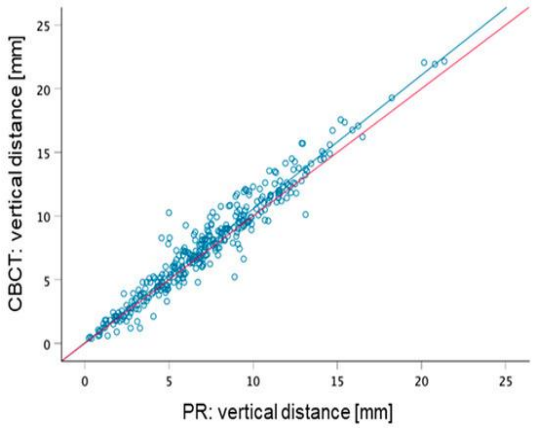

Figure 5. Scatterplot showing the ratio of the vertical measurement distance on CBCT and PAN for the entire dataset (in mm).

When broken down by side, the right maxilla exhibited a mean value of 7.45 ± 3.77 mm using PAN and 7.93 ± 4.16 mm employing CBCT. In the left maxilla, the analogous mean stood at 6.95 ± 3.71 mm on PAN and 7.30 ± 3.94 mm on CBCT. Computing an overall average yielded 7.21 ± 3.74 mm for PAN-based readings and 7.62 ± 4.06 mm for CBCT-based readings. The standard deviation, along with the minimum, maximum, and percentile distribution figures, is presented in **Table 1**.

Table 1. Comparison of corresponding vertical measurements on PAN and CBCT. Mean, standard deviation (SD), maximum, and minimum are expressed in mm.

		N	Mean	SD	Minimum	Maximum	Percentiles		
							25th	50th	75th
Right maxilla	PAN	175	7.45	3.77	0.32	20.16	4.80	7.12	9.52
	CBCT	175	7.93	4.16	0.50	22.05	4.81	7.51	10.31
Left maxilla	PAN	166	6.95	3.71	0.24	21.36	4.38	6.84	9.44
	CBCT	166	7.30	3.94	0.39	22.15	4.28	7.28	9.91
Combined	PAN	341	7.21	3.74	0.24	21.36	4.56	6.96	9.44
	CBCT	341	7.62	4.06	0.39	22.15	4.80	7.35	10.07

To examine the nature of the link between PAN and CBCT data, a two-sided paired-samples t-test was deployed. The mean offset characterizing the paired measurement pairs—derived by taking the PAN value minus the CBCT value in every instance—equaled −0.48 ± 1.07 mm on the right-hand side and −0.35 ± 0.98 mm on the left-hand side. Pooling all matched pairs revealed an average disparity of −0.41 ± 1.03 mm. Moreover, these contrasts between PAN and CBCT were statistically significant, yielding p-values of <0.0001 for the right and left maxillae and the overall set of measurements **(Table 2).**

Table 2. Paired-samples t-test comparing corresponding vertical measurements on PAN and CBCT. Mean, standard deviation (SD), and standard error mean (SEM) are expressed in mm; confidence interval (CI) is expressed as a percentage.

Region	Comparison	Mean difference	SD	SEM	95% CI lower	95% CI upper	t	df	One-sided P	Two-sided P
Maxilla right	Pair 1 (PAN–CBCT)	−0.48	1.07	0.081	−0.64	−0.32	−5.89	174	0.0001	0.0001
Maxilla left	Pair 1 (PAN–CBCT)	−0.35	0.98	0.076	−0.50	−0.20	−4.57	165	0.0001	0.0001
Overall total	Pair 1 (PAN–CBCT)	−0.41	1.03	0.056	−0.52	−0.30	−7.43	340	0.0001	0.0001

Because the p-value alone only confirms whether a statistically detectable phenomenon is present, effect sizes, specifically paired-sample effect sizes, were additionally estimated **(Table 3).** The magnitude of any effect can be calibrated through Cohen's d, under which a value of 0.2 is interpreted as a small effect, 0.5 as a medium effect, and 0.8 as a large or pronounced effect. The average divergences (point estimates) between PAN and CBCT were categorized as weak-to-moderate: right maxilla, d = 0.445; left maxilla, d = 0.355; and the total measurement pool, d = 0.402.

Table 3. Comparison of paired-sample effect sizes for corresponding vertical measurements on PAN and CBCT.

Region	Comparison	Effect size method	Standardizer	Point estimate	95% CI lower	95% CI upper
Maxilla right	Pair 1 (PAN–CBCT)	Cohen's d	1.072	−0.445	−0.600	−0.289
		Hedges' correction	1.076	−0.443	−0.597	−0.288
Maxilla left	Pair 1 (PAN–CBCT)	Cohen's d	0.979	−0.355	−0.511	−0.197
		Hedges' correction	0.983	−0.353	−0.509	−0.196
Overall total	Pair 1 (PAN–CBCT)	Cohen's d	1.028	−0.402	−0.512	−0.292
		Hedges' correction	1.031	−0.402	−0.511	−0.291

The Bravais–Pearson correlation coefficient serves to encapsulate the closeness of the linear relationship shared between the two measurement modalities, with $|R| \leq 0.2$ denoting an absence of correlation, $0.2 < |R| \leq 0.5$ signifying a weak-to-moderate correlation, $0.5 < |R| \leq 0.8$ indicating a clear-to-strong correlation, and $0.8 < |R| \leq 1.0$ reflecting a high or near-perfect correlation. The degree of interdependence linking the vertical measurements on CBCT with those on PAN was deemed high to near-perfect (right maxilla, 0.968; left maxilla, 0.969; combined, 0.969) and reached statistical significance (P = 0.0001).

Bony defects were discernible in 58 out of the overall 341 measurement loci (17%). Of this subset, 33 defects (58.6%) occupied the right maxilla, translating into 10% of the entire measurement count, whereas 25 were situated on the left maxillary side, accounting for 41.4% of the defect observations and representing a 7% fraction of all measurements.

The average recorded extent of osseous defects situated in the right maxilla was 1.73 ± 1.03 mm on PAN compared with 1.85 ± 0.82 mm on CBCT. On the opposing left side, the corresponding mean defect height reached 1.99 ± 1.09 mm under PAN and 2.20 ± 1.19 mm under CBCT **(Table 4).** When all defect-related measurements were combined, the mean height was 1.85 ± 1.05 mm on PAN and 1.99 ± 1.00 mm on CBCT. Details regarding standard deviation, minimum, maximum, and the breakdown across percentiles—including the manner in which individual readings distribute themselves among percentile bands—are enumerated in **Table 4**. These data indicate that the CBCT-derived numbers were modestly superior to those generated via PAN. Additionally, within the 25th percentile band, heights ranged from 1.04 to 1.20 mm on PAN, compared with 1.20 to 1.25 mm on CBCT. For the 50th percentile, the figures ranged from 1.28 to 1.60 mm on PAN and from 1.80 to 2.12 mm on CBCT. Moving to the 75th percentile, the depths extended from 2.41 to 2.93 mm on PAN and from 2.00 to 2.85 mm on CBCT.

Table 4. Descriptive statistics of defect measurements. Mean, standard deviation (SD), maximum, and minimum are expressed in mm.

Region	Measurement type	N	Mean	SD	Minimum	Maximum	25th percentile	Median (50th)	75th percentile
Maxilla right	PAN defects	33	1.74	1.03	0.00	3.84	1.04	1.28	2.41
	CBCT defects	33	1.85	0.82	0.60	4.21	1.25	1.80	2.00
Maxilla left	PAN defects	25	1.99	1.09	0.64	4.00	1.16	1.60	2.93
	CBCT defects	25	2.20	1.19	0.00	4.81	1.20	2.12	2.85
Overall total	PAN defects	58	1.85	1.05	0.00	4.00	1.12	1.60	2.64
	CBCT defects	58	1.99	1.00	0.00	4.81	1.24	1.80	2.42

The box-whisker plot shown in **Figure 6** provides a rapid visual impression that the defect metrics for the left maxilla are marginally greater than those for the right side. The appreciable elongation of whisker elements in the boxplot suggests considerable data dispersion. In the present case, this spread does not follow a Gaussian distribution. Prompted by this deviation from normality, the Wilcoxon matched-pairs signed-rank test was employed.

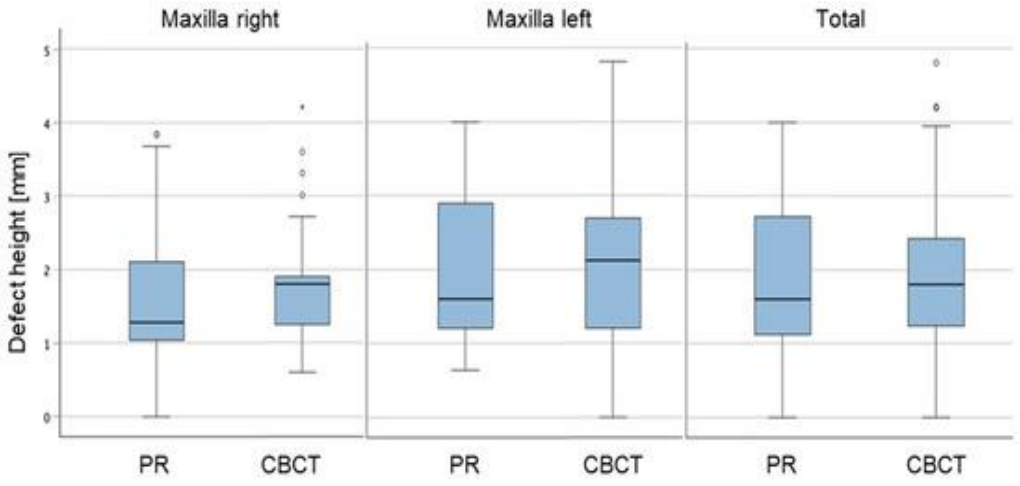

Figure 6. Boxplot diagram illustrating defect measurements. The circles (°) represent outliers, the star (*) represents extreme values.

Owing to the non-normal distribution of the data, statistical significance was assessed using an asymptotic approximation. No statistically discernible differences surfaced when contrasting PAN against CBCT, as reflected by P = 0.228 for the right maxilla, P = 0.119 for the left maxilla, and P = 0.052 for the full collection of defect measurements.

The central objective driving this comparative investigation was to ascertain whether the vertical distance extending from the osseous crest at the first molar down to the antral floor can be measured with equivalent fidelity on matched PAN and CBCT records. In parallel, vertical dimensions within toothless segments of the jaw were assessed. Beyond that, where identifiable within these edentulous spans, the vertical extent of osseous craters was also quantified.

To date, none of the facets explored in the present work have received exhaustive attention in the existing body of literature that employs sizeable, pertinent collections of PAN and CBCT images. For this reason, the study constitutes a novel contribution that may prove instructive when making clinical determinations regarding the planning of implant-borne prosthetic rehabilitations.

Achieving enduring, successful implant restoration hinges upon prosthetically driven, three-dimensional treatment strategizing [23, 24]. Both PAN and CBCT are available to the clinician for diagnostic workup and preoperative preparation before dental interventions [16, 17]. Owing to the inherent dimensions and the spatial arrangement of anatomical structures, not every region of clinical interest can be rendered without ambiguity on PAN images. It may consequently be obscured by various neighboring structures [25].

Published reports attest to the diagnostic preeminence of CBCT over PAN when it comes to discerning anatomical landmarks within the maxilla [19-21]. What is more, CBCT volumes seemingly permit an independent appraisal of anatomic features, insofar as they afford minimal latitude for subjective interpretation of the observations [26]. Against this backdrop, certain authors advocate for a comprehensive three-dimensional radiographic survey of the maxillary sinus before undertaking surgery [20, 21, 27]. Such precaution appears especially warranted whenever substantial bone augmentation is contemplated before fixture insertion within the maxillary sinus territory. Adverse events have been reported with sinus floor elevation procedures [6, 14, 15, 28, 29], and these interventions carry an elevated risk profile when intrasinus septa are encountered [30].

Only a restricted number of studies have scrutinized vertical measurement disparity between CBCT and PAN [26, 28]. In their investigation, Wolff *et al*. [28] noted that although CBCT datasets provided more clinically pertinent information, this additional data did not materially alter the treatment plan, which had already been charted based on the available panoramic radiograph. These conclusions align well with the findings from our own study. The clinical interpretation of PAN-derived findings appears to depend on the evaluating clinician's level of experience. Özalp *et al.* [31] assessed the fidelity of vertical readings obtained from panoramic radiography (PAN) versus cone-beam computed tomography (CBCT) in a study whose design closely mirrored that outlined here, applying a magnification correction factor of 1.2, running counter to what Özalp *et al.* [31] reported—where PAN-based values tended, on average, to exceed those measured on CBCT (by 0.36–0.8 mm)—our own data reveal that PAN readings came out smaller (by 0.35–0.48 mm) than their CBCT counterparts. Taking into account the differences in imaging apparatus and magnification coefficients, coupled with the strong correlational agreement between the two measurement techniques documented in both investigations, it seems reasonable to infer that the magnification factor exerts a considerable influence on the directionality of the observed inter-study discrepancies.

Within their retrospective analysis, Anitua *et al*. [7] appraised the performance of extra-short implant fixtures (≤6.5 mm in length) supporting 15 screw-retained full-arch prostheses situated in the maxilla and mandible. Over a mean surveillance window of 27.2 ± 15.4 months, not a single failure event was registered—neither for the extra-short fixtures themselves nor for the prostheses they supported. On the strength of these observations, the authors endorse the deployment of extra-short implants as a therapeutically equivalent alternative to restorations relying on longer fixtures.

In their narrative synthesis of the literature, Thoma *et al.* [8] compared short and longer implants placed within augmented bone, tracking outcomes up to 18 months following loading with definitive prostheses. Drawing upon the assembled body of evidence encompassed in that review, a mean fixture survival figure of 99.0% was cited for short implants, against 99.5% for long implants inserted into augmented sinus sites, alongside broadly comparable superstructure survival rates. What stands out, however, is the stark contrast in the incidence of surgical complications: 33% for short implants compared with 100% for longer implants subjected to sinus lift procedures.

The findings of a randomized pilot investigation intimated that short implants may, in fact, deliver more favorable outcomes than their longer counterparts placed in previously augmented bone [9]. By the 1-year mark, a statistically significant difference in crestal bone loss around the implants was documented ($P < 0.001$), averaging 1.02 mm for the 6 mm fixtures

compared with 1.09 mm for the 10 mm or greater fixtures.

Storelli *et al.* [32] reported comparable extended-range findings concerning survival and success rates over a decade-long horizon. Marginal bone resorption at the 10-year milestone did not reach statistical significance (P = 0.22), although instances of superstructure debonding were encountered with greater regularity in association with 6 mm implants.

It follows, therefore, that particularly within the posterior maxillary region, an accurate appreciation of true vertical bone height is of paramount importance when weighing the decision as to whether sinus floor elevation is mandated or whether short implants merit consideration.

This very question formed a core line of inquiry in our study, which sought to clarify whether PAN-derived measurements are sufficiently precise or whether recourse to CBCT is indispensable. Although the results yielded statistically significant findings in favor of CBCT, the absolute magnitude of the discrepancy between the two imaging modalities proved exceedingly modest, falling well within clinically tolerable limits: 0.48 mm on the right maxillary side and 0.35 mm on the left. The gap in vertical measurement between these two techniques remained under 2 mm, a finding of practical relevance given the universal dictum in implant dentistry that a safety buffer of 2 mm must be respected. By this logic, the hazard of encroaching upon or violating the maxillary sinus floor when devising a treatment blueprint grounded on panoramic radiographs can be judged to be acceptably low.

To distill the matter, each of the two methods furnishes acceptable accuracy that resides within the 2 mm safety threshold, as borne out by the direct juxtaposition of their outputs. As a consequence, a panoramic X-ray can, in everyday clinical practice, be relied upon to discriminate whether residual bone height is adequate for short implant placement or whether osseous augmentation is required.

Post-extraction remodeling of the alveolar bone frequently gives rise to contour irregularities along the alveolar ridge [33-35]. Breakdown of the hard-tissue scaffold ultimately precipitates the resorption of the overlying soft tissues, thereby undermining treatment outcomes from both aesthetic and biocompatibility perspectives [1]. Additionally, hard-tissue resorption simultaneously drives soft-tissue deterioration, leading to three-dimensional ridge deficiencies that pose considerable reconstructive challenges [13].

The body of research cited above underscores the critical importance of identifying both the presence and magnitude of ridge defects within toothless alveolar segments before implant-borne prosthetic care.

Osseous craters of the alveolar ridge were identifiable in 58 (17%) out of the 341 measurement sites, constituting a comparatively sizeable fraction of edentulous zones that demands attention during the preoperative diagnostic workup. As shown in **Table 4**, the defect magnitudes captured via CBCT were, on average, marginally greater than those recorded on PAN. Even so, these discrepancies were exceedingly trivial and fell short of statistical significance (p = 0.052). On this basis, PAN may likewise be deemed a serviceable diagnostic instrument for gauging the vertical dimension of osseous craters within the toothless jaw territory.

At a fundamental level, CBCT indisputably outperforms PAN in detecting anatomical landmarks. A contributing explanation is that, owing to the intrinsic principles of the imaging technique, only structures within the focal trough are rendered clearly on panoramic radiographs. Anatomic features positioned posterior to the focal trough appear magnified in width, whereas those located anterior to it seem narrowed [18, 25]. Distortions operating in both the horizontal and vertical axes can be encountered beyond the confines of the focal plane. These systematic sources of inaccuracy provide grounds for why measurements taken from PAN images are often regarded as untrustworthy. Malpositioning of the cranium can additionally introduce deformation of the anatomic contours displayed. If the head is misaligned relative to the midsagittal axis, horizontal inaccuracies ensue, such that anatomic elements in the posterior quadrants are portrayed as either broadened or constricted. Deviation of the head from the Frankfort horizontal plane, meanwhile, gives rise to vertical errors, causing structures to appear elongated or foreshortened [18].

Furthermore, CBCT curtails the latitude for interpretive variance, and the findings are comparatively less contingent upon the individual conducting the evaluation [27]. At this juncture, one must note, with a critical eye, that the 25% distortion factor assumed for PAN images could skew the results. Nevertheless, the magnitude of this influence is anticipated to be exceedingly slight, as any such distortion was kept to a minimum through periodic quality assurance protocols encompassing both servicing and calibration against physical objects of established dimensions. This consideration applies equally to radiographs sourced from external facilities. In upwards of 70% of the externally acquired images, dimensional reference objects were visible, suggesting

that adequate image calibration had been achieved. That said, CBCT is not without its own shortcomings, among them the emergence of artifacts. This concern becomes especially pronounced when metallic restorations or root canal filling materials occupy the zone under examination [36]. An additional well-known pitfall of CBCT is motion artifacts resulting from insufficient cranial stabilization during acquisition. The exposure duration required to generate a CBCT dataset can also be a contributing factor. For this reason, CBCT protocols employing a restricted field of view centered on the region of clinical interest, thereby shortening acquisition times, present a distinct advantage over those utilizing larger FOVs [37].

Within the confines of the present investigation, a single examiner first interpreted the panoramic radiographs, then evaluated the CBCT datasets following a minimum 14-day hiatus. A higher level of statistical significance might have been achieved had more examiners participated in the evaluation. Having said that, the strong intra- and inter-rater consistency established during the study's preliminary phase lends considerable weight to the findings' trustworthiness.

All measurements performed on PAN images accounted for a uniform magnification correction factor (1.25), a consistently demarcated measurement zone, and the use of two identical anatomical landmarks. While recruiting an adequately sized study sample reduces the likelihood that these variables will systematically skew the outcomes, they nonetheless remain potential sources of error. Given the retrospective character of this work, such influences lay beyond the investigators' control. It is also worth noting that the computed value (1.25) is cited in the scientific literature, where it is presented both as a conventional scaling coefficient for panoramic imaging and as a calibration benchmark [38].

The misgivings routinely attached to panoramic radiography would seem to have exerted only a marginal bearing upon our study. The slight measurement differences between PAN and CBCT images might also be attributed to the deliberate selection of correctly executed panoramic exposures (see the inclusion criteria).

Since CBCT examinations entail a considerably greater burden of ionizing radiation compared with conventional panoramic radiography, CBCT should be reserved strictly for circumstances in which the anticipated diagnostic yield for the patient justifies the added exposure risk. Such a stance aligns squarely with the ALARA principle (As Low As Reasonably Achievable) [39]. The substantially higher financial outlay associated with CBCT scanning also warrants due consideration. Added to this is the fact that panoramic radiographic apparatus enjoys far broader distribution across clinical facilities than does CBCT hardware. Taken together, these considerations further buttress the case for panoramic radiography as a reliable method for vertical measurements in the posterior maxillary region [40].

Turning to the original hypothesis, which posited that VD and DH measurements are captured with equal fidelity on CBCT and PAN images alike, this premise must be set aside. Still, the data reveal that the disparities between the two imaging modalities are exceedingly minor and remain well within the clinical acceptability envelope.

It was never the objective of this work to explore the spatial envelope available for accommodating an implant fixture, but rather to draw a direct comparison between PAN and CBCT through vertical dimensional assessment. Subsequent investigations could take up this line of inquiry, probing both the vertical and horizontal spatial prerequisites for implant placement.

The quantification of osseous defects in this study did not yield any statistically significant results. Nonetheless, this finding warrants circumspect interpretation given the modest sample size and the absence of full standardization. For forthcoming research endeavors, it would be prudent to draw upon a substantially expanded corpus of radiographic images.

Conclusion

Diminished alveolar ridge stature, together with ridge concavities, is acknowledged as the foremost constraining factor in posterior maxillary reconstruction. This reality underscores the need for precise quantification of the vertical dimension below the maxillary sinus floor.

Drawing upon the body of evidence put forward herein, the authors arrive at the judgment that the divergences between PAN- and CBCT-based measurements of the vertical span from the alveolar crest to the antral floor are negligible. Consequently, PAN may be regarded as a trustworthy modality for diagnostic appraisal and the determination of vertical bone height in the posterior maxilla.

Acknowledgments: None

Conflict of Interest: None

Financial Support: None

Ethics Statement: None

References

1. Buser D, Chappuis V, Belser UC, Chen S. Implant placement post extraction in esthetic single tooth sites: When immediate, when early, when late? Periodontol 2000. 2017;73(1):84-102.
2. Tonetti MS, Hämmerle CH; European Workshop on Periodontology Group C. Advances in bone augmentation to enable dental implant placement: Consensus Report of the Sixth European Workshop on Periodontology. J Clin Periodontol. 2008;35(Suppl 8):168-72.
3. Aghaloo TL, Moy PK. Which hard tissue augmentation techniques are the most successful in furnishing bony support for implant placement? Int J Oral Maxillofac Implants. 2007;22(Suppl):49-70. Erratum in: Int J Oral Maxillofac Implants. 2008;23(1):56.
4. Khoury F, Schmidt C, Jackowski J. The influence of suturing and or gluing of perforated Schneiderian membrane during sinus lift procedure on the outcome: A retrospective study. Int J Implant Dent. 2024;10(1):48.
5. Pjetursson BE, Tan WC, Zwahlen M, Lang NP. A systematic review of the success of sinus floor elevation and survival of implants inserted in combination with sinus floor elevation. J Clin Periodontol. 2008;35(Suppl 8):216-40.
6. Zijderveld SA, van den Bergh JP, Schulten EA, ten Bruggenkate CM. Anatomical and surgical findings and complications in 100 consecutive maxillary sinus floor elevation procedures. J Oral Maxillofac Surg. 2008;66(7):1426-38.
7. Anitua E, Eguia A, Alkhraisat MH. Extra-short implants (≤6.5 mm in length) in atrophic and non-atrophic sites to support screw-retained full-arch restoration: A retrospective clinical study. Int J Implant Dent. 2023;9(1):29.
8. Thoma DS, Haas R, Sporniak-Tutak K, Garcia A, Taylor TD, Tutak M, et al. Randomized controlled multi-centre study comparing shorter dental implants (6 mm) to longer dental implants (11-15 mm) in combination with sinus floor elevation procedures: 10-year data. J Clin Periodontol. 2024;51(5):499-509.
9. Pistilli R, Felice P, Cannizzaro G, Piatelli M, Corvino V, Barausse C, et al. Posterior atrophic jaws rehabilitated with prostheses supported by 6 mm long 4 mm wide implants or by longer implants in augmented bone. One-year post-loading results from a pilot randomised controlled trial. Eur J Oral Implantol. 2013;6(4):359-72.
10. Esquivel J, Meda RG, Blatz MB. The Impact of 3D Implant Position on Emergence Profile Design. Int J Periodontics Restorative Dent. 2021;41(1):79-86.
11. Pelekos G, Chin B, Wu X, Fok MR, Shi J, Tonetti MS. Association of crown emergence angle and profile with dental plaque and inflammation at dental implants. Clin Oral Implants Res. 2023;34(10):1047-57.
12. Jose EP, Paul P, Reche A. Soft Tissue Management Around the Dental Implant: A Comprehensive Review. Cureus. 2023;15(10):e48042.
13. Puisys A, Janda M, Auzbikaviciute V, Gallucci GO, Mattheos N. Contour angle and peri-implant tissue height: Two interrelated features of the implant supracrestal complex. Clin Exp Dent Res. 2023;9(3):418-24.
14. Fayek MM, Amer ME, Bakry AM. Evaluation of the posterior superior alveolar artery canal by cone-beam computed tomography in a sample of the Egyptian population. Imaging Sci Dent. 2021;51(1):35-40.
15. Hung K, Montalvao C, Yeung AWK, Li G, Bornstein MM. Frequency, location, and morphology of accessory maxillary sinus ostia: A retrospective study using cone beam computed tomography (CBCT). Surg Radiol Anat. 2020;42(2):219-28.
16. Kämmerer PW, Thiem D, Eisenbeiß C, Dau M, Schulze RK, Al-Nawas B, et al. Surgical evaluation of panoramic radiography and cone beam computed tomography for therapy planning of bisphosphonate-related osteonecrosis of the jaws. Oral Surg Oral Med Oral Pathol Oral Radiol. 2016;121(4):419-24.
17. Friedland B, Metson R. A guide to recognizing maxillary sinus pathology and for deciding on further preoperative assessment prior to maxillary sinus augmentation. Int J Periodontics Restorative Dent. 2014;34(6):807-15.
18. Lurie AG. Panoramic Imaging. In: White SC, Pharoah MJ, editors. Oral Radiology: Principles and Interpretation. 5th ed. Shanghai: Mosby; 2004. p. 191-209.
19. Crockett B, Broome A, Tawil P, Tyndall D. Comparison of incidental findings on cone beam computed tomographic and 2-dimensional images. Gen Dent. 2023;71(5):64-71.
20. Fukuda M, Matsunaga S, Odaka K, Oomine Y, Kasahara M, Yamamoto M, et al. Three-dimensional analysis of incisive canals in human

dentulous and edentulous maxillary bones. Int J Implant Dent. 2015;1(1):12.
21. Ketabi AR, Hassfeld S, Lauer HC, Piwowarczyk A. The comparison of visibility of the maxillary sinus septa between cone-beam computed tomography scans and panoramic radiograph images as dependent on the cortical bone thickness: A retrospective comparative study. Int J Implant Dent. 2024;10(1):23.
22. World Medical Association. World Medical Association Declaration of Helsinki: Ethical principles for medical research involving human subjects. JAMA. 2013;310(20):2191-4.
23. Chen Z, Li J, Sinjab K, Mendonca G, Yu H, Wang HL. Accuracy of flapless immediate implant placement in anterior maxilla using computer-assisted versus freehand surgery: A cadaver study. Clin Oral Implants Res. 2018;29(12):1186-94.
24. Cooper LF, De Kok IJ, Thalji G, Bryington MS. Prosthodontic Management of Implant Therapy: Esthetic Complications. Dent Clin North Am. 2019;63(2):199-216.
25. Shiki K, Tanaka T, Kito S, Wakasugi-Sato N, Matsumoto-Takeda S, Oda M, et al. The significance of cone beam computed tomography for the visualization of anatomical variations and lesions in the maxillary sinus for patients hoping to have dental implant-supported maxillary restorations in a private dental office in Japan. Head Face Med. 2014;10:20.
26. Malina-Altzinger J, Damerau G, Grätz KW, Stadlinger PD. Evaluation of the maxillary sinus in panoramic radiography-a comparative study. Int J Implant Dent. 2015;1(1):17.
27. Lana JP, Carneiro PM, Machado Vde C, de Souza PE, Manzi FR, Horta MC, et al. Anatomic variations and lesions of the maxillary sinus detected in cone beam computed tomography for dental implants. Clin Oral Implants Res. 2012;23(12):1398-403.
28. Wolff C, Mücke T, Wagenpfeil S, Kanatas A, Bissinger O, Deppe H, et al. Do CBCT scans alter surgical treatment plans? Comparison of preoperative surgical diagnosis using panoramic versus cone-beam CT images. J Craniomaxillofac Surg. 2016;44(10):1700-5.
29. Maridati P, Stoffella E, Speroni S, Cicciu M, Maiorana C. Alveolar antral artery isolation during sinus lift procedure with the double window technique. Open Dent J. 2014;8:95-103.
30. Wen SC, Chan HL, Wang HL. Classification and management of antral septa for maxillary sinus augmentation. Int J Periodontics Restorative Dent. 2013;33(4):509-17.
31. Özalp Ö, Tezerişener HA, Kocabalkan B, Büyükkaplan UŞ, Özarslan MM, Şimşek Kaya G, et al. Comparing the precision of panoramic radiography and cone-beam computed tomography in avoiding anatomical structures critical to dental implant surgery: A retrospective study. Imaging Sci Dent. 2018;48(4):269-75.
32. Storelli S, Abbà A, Scanferla M, Botticelli D, Romeo E. 6 mm vs 10 mm-long implants in the rehabilitation of posterior jaws: A 10-year follow-up of a randomised controlled trial. Eur J Oral Implantol. 2018;11(3):283-92.
33. Mecall RA, Rosenfeld AL. Influence of residual ridge resorption patterns on implant fixture placement and tooth position. 1. Int J Periodontics Restorative Dent. 1991;11(1):8-23.
34. Thoma DS, Mühlemann S, Jung RE. Critical soft-tissue dimensions with dental implants and treatment concepts. Periodontol 2000. 2014;66(1):106-18.
35. Couso-Queiruga E, Stuhr S, Tattan M, Chambrone L, Avila-Ortiz G. Post-extraction dimensional changes: A systematic review and meta-analysis. J Clin Periodontol. 2021;48(1):126-44.
36. Suomalainen A, Pakbaznejad Esmaeili E, Robinson S. Dentomaxillofacial imaging with panoramic views and cone beam CT. Insights Imaging. 2015;6(1):1-16.
37. Schulze R, Heil U, Gross D, Bruellmann DD, Dranischnikow E, Schwanecke U, et al. Artefacts in CBCT: A review. Dentomaxillofac Radiol. 2011;40(5):265-73.
38. Tronje G, Eliasson S, Julin P, Welander U. Image distortion in rotational panoramic radiography. II. Vertical distances. Acta Radiol Diagn. 1981;22(4):449-55.
39. ICRP Publication 105. Radiation protection in medicine. Ann ICRP. 2007;37(1-6):1-63.
40. Hayashi T, Arai Y, Chikui T, Hayashi-Sakai S, Honda K, Indo H, et al. Clinical guidelines for dental cone-beam computed tomography. Oral Radiol. 2018;34(2):89-104.